Tunneling study of localized bands in superconductors with magnetic impurities (normal Kondo alloys in the superconducting proximity)*

L. Dumoulin, E. Guyon, and P. Nedellec
Laboratoire de Physique des Solides,† Université Paris-Sud, 91405 Orsay, France
(Received 28 April 1976)

We present an experimental study of the magnetic behavior of dilute CuX (X = Mn, Cr, Fe) and AuFe alloys using superconducting electron tunneling. Superconductivity is induced by overlaying the normal alloy film with a superconducting Pb one. The most important result of this study is the existence of localized states, within the superconducting energy gap of the sandwich, their position in energy being characteristic of the nature of the impurity and their amplitude being related to its concentration. This localized band had been predicted from the Müller-Hartmann and Zittartz (MHZ) theory which calculates, going beyond the first Born approximation, the scattering of conduction electrons by magnetic impurities. Initially this paper emphasizes the conditions in which a quasi-BCS approach, neglecting the spatial variation of the order parameter, can be used in the tunneling experiments. The characteristics of the impurity band are discussed systematically in the CuCr case. Systematic results on materials of various Kondo temperatures are presented. The agreement with the MHZ approach deteriorates as the Kondo temperature increases and strong-coupling effects should be considered. The possibility of using this technique as a new tool for sensitive spectroscopic analysis is suggested.

I. INTRODUCTION

Superconductivity is a very sensitive tool for the study of dilute magnetic impurities in various matrices, since magnetic interactions destroy the superconductive pairing. Excellent reviews, both experimental[1a,b] and theoretical,[1c] can be found on this subject. The superconducting proximity effect obtained by overlaying a nonsuperconducting film with a superconductor makes it possible to induce superconductivity in nonsuperconducting alloys.[2] In a first article,[3] measurements of the critical temperatures of CuX-Pb bilayers (X = Cr, Mn, Fe, Co) have led to a determination of the magnetic depairing energy of the impurities: $\Gamma(c, T)$. A detailed description of the metallurgical and normal-state properties of these systems has been given in this first paper. We extend here the proximity method to the study of the tunneling density of states obtained on the alloy side of similar bilayers. In a recent letter,[4] we have shown that tunneling can show the existence of an impurity band due to localized excited states (LES) within the superconducting gap. This article reports an extended discussion as well as systematic experiments centered around this point. The existence of LES was first predicted by theoretical analysis beyond the level of the Abrikosov and Gor'Kov (AG) first Born approximation.[5] However, experimental tunneling studies previous to our work[1] and using homogeneous superconductors alloys with 3d or Ce impurities, have only shown that the densities of states within the gap were larger in that case then predicted by AG. This enhancement agrees with the γT term observed in the specific heat of those alloys.[1b]

Woolf and Reif[6] were the first to observe such a deviation in their tunneling experiments on homogeneous alloys of the 3d transition elements, although their results with Gd impurities followed well the gapless density of states predicted by AG. The enhancement of the gapless behavior for concentrated alloys can be understood as a limit of the localized bands formed when the LES wave function overlap strongly. In our experiments, with a large enough resolution and using low-concentration alloys, we have been able to see the development of localized-band states. The proximity effect permits the study of the superconducting properties of various alloys (covering a wide range of T_K values) and also provides an original tool to vary the effective superconducting critical temperature for a given magnetic alloy while keeping the magnetic properties and concentration constant. Comparison is made with the Müller-Hartmann and Zittartz theory.[1c] Great attention is paid to the control of the quality of tunneling samples (Chap. II) and to the validity of the approximation made in the application of a theory, introduced for homogeneous alloys on inhomogeneous proximity effect sandwiches (Sec. III).

We devote an appreciable part of this article to these preliminary considerations which are fundamental for the quantitative analysis of our results. The reader interested only in the impurity bands study can go directly to Sec. III E. A rather complete study of the CuCr-Pb system (Chap. IV) allows us to describe experimentally the characteristics of the impurity bands within the gap: its *height* and *width* which grow as the concentration

increases; its *location*, related to the ratio of the Kondo temperature T_K, characteristic of the magnetic alloy to the effective critical temperature T_c^* characteristic of the induced superconductivity. In Chap. V we present results on materials of different T_K. In the conclusion, we discuss the validity of the Müller-Hartmann and Zittartz theory used throughout the experimental discussion.

II. PREPARATION AND CONTROLS OF SAMPLES

Figure 1(a) shows a section of a typical tunneling junction. The first electrode, 1, is normal (Al above 1.5 °K; Mg; *Al*-5-at.% Mn) or superconducting (Al below 1.5 °K) film. The second electrode, 2, is a magnetic alloy film, *CuX*, overlayed by a Pb film which induces superconductivity in the *CuX*. The preparation and control of the sandwiches, discussed in our previous work (3), will be summarized in Sec. IIA. We shall discuss in more detail the preparation (Sec. IIB) and control (Sec. IIC) of tunneling junctions.

A. *CuX*; *CuX*-Pb: Preparation and properties

CuX films are prepared by evaporation in ultrahigh vacuum (pressure less than 10^{-8} Torr) of the alloy. We use a single-ingot source for *Cu*Cr and *Cu*Fe. The concentration is uniform across the film thickness. *Cu*Mn shows a strong distillation effect if it is prepared from a single source. A flash evaporation technique has been used in the present experiments. Pellets of $\frac{1}{10}$ mm^3 of the alloy are evaporated one by one. Each grain contributes for about 15 Å to the total film thickness.

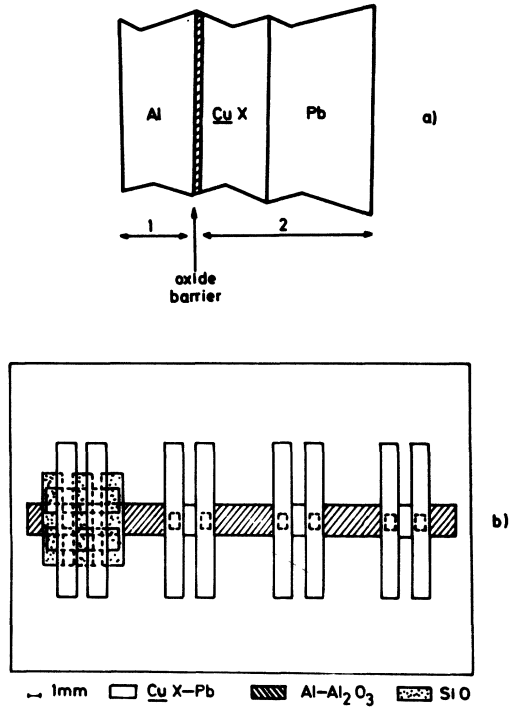

FIG. 1. (a) Transverse view of a typical junction used for the study of the normal-side-tunneling density of states of bilayers. (b) Top view of a sample (four pairs of junctions)—strips of SiO (shown only on one pair of junctions) define windows on the oxide barrier.

Resistive measurements of the films lead to a determination of thickness and impurity concentration. The low-temperature variation of the resistivity shows the resistance minimum associated with the Kondo effect, exactly as in the corresponding bulk alloys. It is very reasonable to assume that the bulk magnetic properties, and in particular the T_K values, persist in our films. Unlike the films prepared from a single source (see Ref. 3), *Cu*Mn films prepared by flash evaporation technique show the correct bulklike behavior.

The Cu-Pb pair is a good candidate for the proximity effect (no interdiffusion at room temperature, no intermetallic compound). We have also used the Au-Pb combination where the possible formation of intermetallic compounds is prevented by preparing and always keeping the samples at a temperature below-100 °C. The residual mean free path in the normal state of the films studied here is always larger than the thickness for all materials.

B. Preparation of the tunnel junctions

A longitudinal film [see Fig. 1(b)] is first evaporated on the glass substrate. The tunneling barrier is formed by glow-discharge oxidation of this first electrode, during a few minutes, in a dry atmosphere of pure oxygen at a pressure around 5×10^{-2} Torr. The area of the tunneling junction formed on this barrier is limited by a window obtained by the evaporation of strips of SiO. Spurious effects arising from the improper superposition of the *CuX* and Pb films which are wider than the opening of the window, are thus eliminated. We have also noted an improvement in the quality of the junctions made by this technique (suppression of the edge effects on both electrodes). A typical sample, illustrated in Fig. 1(b), consists of four pairs of junctions. The two junctions of a pair are identical. The four pairs differ in the second electrode (different *CuX* material or normal film thickness). Three different tunneling samples can be prepared in a single run. They differ, for example, in the material for the first electrode (Al, Mg, *Al*-5-at.% Mn). On the fourth sample, we prepare the test films (*CuX* or Pb single films) and the sandwiches used for resistive T_c measurements.

C. Control of the junctions

The usual measurement of the junction resistance R_j uses the four branches of the two films as the four electrodes. This is a correct four-terminal measurement if the resistance of the films is much smaller than the junction one,[7] which is the case, within a 1% accuracy, for our junctions on Al and *Al*Mn at all temperatures ($R_j \simeq 100\ \Omega$). For Mg junctions of smaller resistance ($R_j \simeq 0.1\ \Omega$), a typical error of less than 5% can be introduced. In the following, we call $\sigma(V,T)$ the normalized conductance of a junction at a bias V and temperature T. It is the ratio of the dynamical conductance $R(V)^{-1} = (dI/dV)$ in the superconducting state, to the value at low temperature with both the electrodes in the normal state.

The tunneling conductance $\sigma_T(V,T)$ can differ from the measured conductance $\sigma_M(V,T)$ because of the spurious conductance $\sigma_p(V,T)$. In order to estimate the accuracy of σ_T, it is important to have an upper limit for σ_p. It is generally admitted that the origin of σ_p is the existence of partially superconducting metallic bridges in parallel with the tunneling path. Their superconducting part can become normal by a critical current effect, when V increases. From this picture, it is obvious that $\sigma_p(V,T)$ is a decreasing function of V and T. An upper limit for σ_p is $\sigma_M(0, T_{\min})$, where $T_{\min}$ is the lowest temperature of the experiment.

(a) If the tunneling conductance has a strong minimum at zero bias, the value $\sigma_M(0, T_{\min})$ gives an accurate upper limit for σ_p. This is the case, if S has a true energy gap at $T_{\min} \ll T_c$: for example, if S is a BCS superconductor, $\sigma_T(0,T) \simeq 10^{-2}$, when $T \simeq 0.25\ T_c$. We speak of "good junctions" when $\sigma_p < 10^{-2}$.

(b) When the density of states of S exhibits only small variations, as in the gapless-limit situation, this test is not sensitive enough. We have developed the following method: we measure accurately the junction resistances at room temperature R_A and at low temperature in the normal state R_H; the ratio $P = R_H/R_A$ is larger than 1: the thermal excitation effect, which contributes to the current at high T, disappears at low T while the tunneling current remains independent of T. For a given series of "good" [as defined in (a)] junctions, prepared and studied simultaneously, *P is constant within* 1%, independently of R_A ($10 < R_A < 100\ \Omega$) and of the nature of X in CuX (in the concentration range used, $c < 500$ ppm). P varies with the nature of the first electrode (it varies typically from 1.25 to 1.30 from pure Al to *Al*-5-at.% Mn and weakly with ageing, but in the same way for all the junctions of a series. In "bad" junctions of a given sample, P is smaller because the resistance of the metallic bridges is an increasing function of T. A "good" (criterion *a*) test junction is used to give the value of P, for a given sample. If another junction has a value of P smaller by more than 2%, it is considered as "bad" and is not used. This second test can only be used for large enough tunnel resistance (case of Al and *Al*Mn) and turns out to detect "bad" junctions which have a conductance in parallel σ_p larger than 0.03. Another obvious test of quality is the reproducibility in the two identical sandwiches of a pair. From the different controls on the junctions, we can estimate the absolute accuracy in the normalized conductance results to better than 0.03.

III. TYPICAL RESULTS AND MAIN LINES OF ANALYSIS

The dynamical resistance of the junctions is obtained using a standard current modulation technique.[8] Figure 2(a) gives the general shape obtained for CuX-Pb sandwiches. The strong variation of $\sigma(V)$ around 1 mV is associated with an induced energy gap in CuX. Outside the gap, structures of magnitude (2–3)% are observed around the Pb phonon energies. This shows the nonlocal character of the superconducting interaction: the Pb phonons are seen by "transparency" through the CuX film.[9] The shape above the gap is identical for CuX-Pb and Cu-Pb and we have not been able to detect any significant additional structure above the gap in the CuX-Pb case. Figure 2(b) shows $R(V)$ inside of the gap of a CuCr-Pb sandwich. The original feature, as compared with the Cu-Pb case [see, for example, $\sigma(V)$ on Fig. 4] is the existence of a resistance minimum within the gap. We shall briefly recall in Sec. III A the connection between $\sigma(V,T)$ and the superconducting density of states. In Sec. III B we present experimental proofs that the observed structure is a bulk density-of-states property and not a barrier effect. We shall summarize in Sec. III C the Müller-Hartmann and Zittartz theory (homogeneous alloy with a BCS matrix). We give in Sec. III D the approximation made in the application to the proximity effect geometry.

A. Tunneling conductance and density of states

The tunneling conductance using a normal first electrode is related to the normalized density of states $D(E,T)$ at energy E by

$$\sigma(V,T) = \frac{1}{2}\frac{d}{d(eV)} \int_0^\infty D(E,T)[\tanh\beta'(E+eV) - \tanh\beta'(E-eV)]\,dE\,, \tag{1}$$

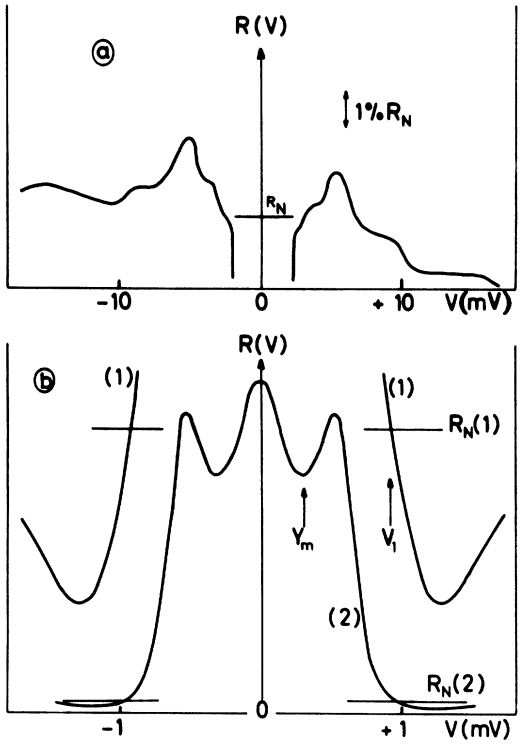

FIG. 2. (a) General shape, outside the gap, of the tunneling resistance $R(V)=dV/dI(V)$ at 0.95 °K, on *Cu*-Pb or *CuX*-Pb sandwiches. The resistance of the junction in the normal state of both the electrodes, R_N, is deduced within 1% accuracy from the interpolation of the background at high voltage. (b) Dynamical resistance of a junction Mg-MgO-*Cu*Cr (150 Å, 10 ppm)/Pb (1000 Å) at 0.95 K. Curve (1) details the gap edge and gives accurately $V_1[R(V_1)=R_N]$; curve (2) shows the minimum of the resistance at Y_m associated with the impurity band. The curve is symmetric in positive and negative bias.

where $\beta'=\frac{1}{2}k_BT$; k_B is the Boltzmann constant. At zero temperature $\sigma(V,0)$ is identical to $D(V,0)$. For $T\neq 0$, $\sigma(V,T)$ is approximately an average of $D(V+\Delta E,T)$, where $-3k_BT\lesssim\Delta E\lesssim 3k_BT$. The use of a superconducting first electrode of gap Δ_1 reduces the Fermi-distribution effect and the resolution at a given temperature is improved.[10] In this work however we have not used this possibility much, because other structures can be observed below the gap in tunneling between two superconductors (subharmonic structures, Josephson effect).

B. Results are free of barrier effects

The previous formula (1) is valid for purely elastic tunneling and neglects deviations (like inelastic tunneling effects) caused by inhomogeneous distribution of impurities close to or inside the barrier.[11] The connection of the so called zero-bias anomalies around $V=0$ with an energy-dependent magnetism, has been established experimentally without ambiguity only in a few cases. The use of these results for the better understanding of magnetism has been rather limited and frustrating. This was due in part of the difficulty of controling, with enough accuracy, the exact distribution near the barrier of the impurities which, as discussed theoretically,[12] is an essential factor.

Zero-bias anomalies are observed in the normal state of the electrodes. Here the resistance minimum peak is intrinsically related to bulk superconductivity: (i) no tunneling structure was observed in tunneling on single *CuX* films of low enough concentration of *X* to prevent segregation of the alloy[13]; (ii) the structure disappears when superconductivity is quenched (above T_c or in a large enough magnetic field); (iii) the structure is no longer resolved above a temperature (still smaller than T_c) which depends on the induced energy-gap magnitude. Thus, an interpretation in terms of a barrier anomaly is not possible.

An interdiffusion of the two materials in proximity can cause some anomalies within the gap in bad sandwiches.[14] We have never observed any anomaly below the energy gap of Cu-Pb sandwiches. The shape of the curves with *CuX*-Pb is not modified after a long storage (a week) at room temperature.

Let us note finally the identity of the results when the same second electrode was deposited at the same time on junctions formed on Mg and Al-5-at.% Mn. This again shows the nature of the tunneling barrier is unimportant.

C. Müller-Hartmann and Zittartz theory (Ref. 1c)

This theory represents the most complete description of the density of states, within the frame of perturbation treatments, of the $-J\vec{S}\cdot\vec{s}$ Hamiltonian in superconductors. It is consistent with other theoretical description.[15] We shall use it to analyze our experimental results.

The starting point assumes a spin S at the impurity site with an infinite lifetime and describes its interaction with the conduction electrons of spin $\vec{s}$ by an Hamiltonian $-J\vec{S}\cdot\vec{s}$, where J is an exchange energy. The perturbative treatment of this interaction to order J^2, made by Abrikosov and Gorkov[5,16] (AG) is the basic description of a superconductor with paramagnetic impurities. The matrix is a BCS superconductor characterized by only one parameter $\Delta^B(0)$, which is the value of the order parameter as well as the energy gap at $T=0$. The alloy is described by an order pa-

rameter Δ which differs from the energy gap ω_g. Both are temperature and impurity concentration dependent via a depairing energy parameter

$$\Gamma_{AG} = \tfrac{1}{2}\pi c N_0 J^2 S(S+1) .$$

c is the concentration of impurities of spin S and N_0 the electronic density of states at the Fermi level. Figure 3(a) gives the shape of the density of states for different concentrations. The gapless situation is shown.

The treatment of the interaction $-J\vec{s}\cdot\vec{S}$ to orders higher than J^2 gives significant deviations from the above results. It leads to the existence of localized excited states in the gap (LES) as pointed out by Shiba[17] using a classical spin ($S \to \infty, JS$ finite) treatment or starting directly from the Anderson Hamiltonian.[18] Shiba's approach does not include the Kondo effect since it neglects transverse part of the moment. In a Kondo superconducting alloy, the electrons are influenced by two competitive mechanisms: the screening of the spin which involves the characteristic energy $N_0 J$ and the pairing characterized by the energy $N_0 V$ of the superconducting matrix. Below T_c, this latter term replaces $k_B T$ which controls the temperature dependence of the magnetism in the normal state of the alloy. In this description, T_K is defined by

$$T_K = T_F e^{1/N_0 J} \quad (J<0) .$$

As a result of the above competition, the parameter $\tau = \ln(T_K/T_c)$ will play the central role.

The scattering amplitude of quasiparticles by one impurity has two poles at energies $\pm\omega_0$ ($\omega_0 = y_0\Delta$). The corresponding density of states $n(\omega)$ expressed as a function of the energy ω is given by

$$n(\omega) = -\tfrac{1}{2}[\delta(\omega-\Delta)+\delta(\omega+\Delta)] + \tfrac{1}{2}\alpha[\delta(\omega-\omega_0)+\delta(\omega+\omega_0)] + n_{cont}(\omega) . \quad (2)$$

Half a state per impurity is taken from each gap edge and $\frac{1}{2}\alpha$ states appear at energies $\pm\omega_0$, while a continuum contribution n_{cont} is added to the BCS distribution. The density of states is symmetric around the Fermi level. The location y_0 of the LES was calculated analytically ($T \to T_c$ limit) and also numerically ($T=0$ limit): y_0 is close to 1 when J is positive or when it is negative but with an absolute value much smaller than the pairing potential V. The latter case, which corresponds to $T_K \ll T_c$ is nothing but the AG limit in which the LES is indeed indistinguishable from a depression of the gap edge towards low energies. In the limit $T \to T_c$ and $J<0$, y_0 is given by

$$1 - y_0^2 = \pi^2 S(S+1)/[\ln(T_K/T_C) + \pi^2 S(S+1)] . \quad (3)$$

When the ratio T_K/T_c increases, the LES crosses into the gap: it is in the middle of the gap for $T_K = T_c$. In this calculation ($T \to T_c$), α in formula (2) is equal to 1. Figures 12(a) and 12(b) give the calculated values of y_0 and α in the limit $T=0$ for $S=\frac{1}{2}$. The terms neglected in the $T \to T_c$ limit depend on $\Delta(T)/k_B T$. Because most of variation of Δ with T is near T_c, the $T=0$ limit is obtained not too far below T_c and would be the more realistic situation for comparison with experiments, carried out at low temperature to reduce the thermal smearing. However, the simpler T_c limit gives good account for the main features of the impurity band and we shall use it as a first approach.

At finite concentration, the wave functions arising from the different impurities overlap and give a band of allowed states within the initially forbidden energy range. The shape of the bands was calculated by Zittartz, Bringer, and Müller-Hartmann[19] (ZBMH) for $T \to T_c$. It is completely determined by Δ, y_0, and $\bar{c} = c/(2\pi N_0 \Delta)$. Typical shape of the density of states is given Fig. 3(b). Δ must be renormalized to take into account the effect of the finite concentration c. At low $\bar{c}$, the density of states $N(\omega)$ is

$$N(\omega) = \tfrac{1}{2}(1-y_0^2)^{-3/2}[2\bar{c}(1-y_0^2)^{3/2} - (y-y_0^2)]^{1/2} , \quad (4)$$

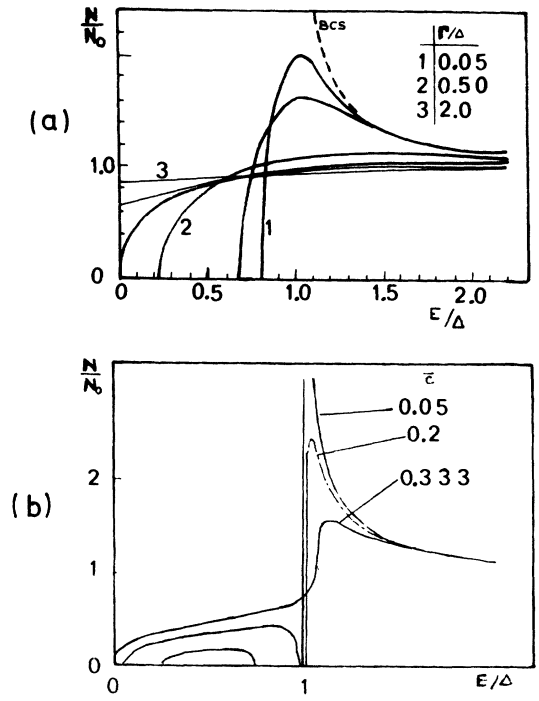

FIG. 3. Density of states a superconductor with different concentrations of magnetic impurities: (a) in the AG picture, from Ref. 16; (b) in the Müller-Hartmann and Zittartz picture from Ref. 19: a localized band around the energy $E = y_0\Delta$ is predicted. Here $y_0 = 0.5$.

so that the width and the height of the band are both proportional to $\sqrt{c}$. The solution for all values of $\bar{c}$ was obtained using a computed calculation provided to us by Bringer.

D. Quasi-BCS-approximation

The ZBMH calculation summarized above applies to a homogeneous alloy with a BCS matrix. At the present time, there is no similar calculation in the proximity effect situation. Such an extension was made by Kaiser and Zuckermann[20] using the MacMillan model for the proximity effect,[21] but applied only if the impurities in the normal film follow the AG description. As far as the depression of the critical temperature is concerned,[3] it is possible to discuss the deviation from the AG predictions in terms of an effective pair-breaking parameter Γ_{eff} and to compare it with the Müller-Hartmann and Zittartz theory.

Here we are dealing with a qualitatively new effect as compared with the AG result—the presence of LES within the gap—and it is no longer possible to use a similar extension.

We use a quasi BCS approximation which assumes that: (i) Cu films in proximity behave as BCS superconductors, in particular as far as the excitation spectrum measured by a tunneling experiment is concerned. (ii) If we add dilute magnetic impurities, the CuX alloy retains its usual Kondo temperature. This second point is rather obvious. The interaction between impurities and conduction electrons is local. In the normal state of the bilayer, it is insensitive to the presence of Pb in contact with the Cu matrix.

The first point may appear as a drastic approximation because of the spatial variation of the order parameter in proximity effect geometry. However, this approximation is reasonable in our present experiments because of the following:

(a) The normal films N are much thinner than the characteristic length of the induced superconductivity. Thus, the superconducting order parameter in N is nearly constant across the thickness: all impurities experience the same order parameter.

(b) The films are clean (the residual electronic mean free path is larger than the thickness) and we are interested by tunneling results in N. Tunneling in clean materials is rather selective in direction and measures a nearly-one-dimensional density of states corresponding to excitations travelling perpendicular to the barrier. It is insensitive to the anisotropy of the excitations.

(c) The tunneling density of states for Cu-Pb is close to the BCS one.

Figure 4 shows the dynamical conductance $\sigma(V)$

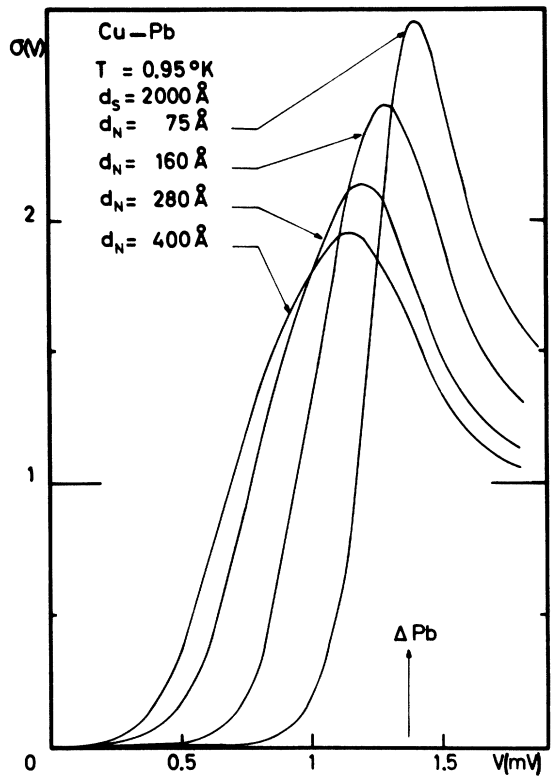

FIG. 4. Tunneling conductances on Cu-Pb sandwiches of the same Pb film thickness and various Cu films thicknesses.

obtained on a series of samples of a given thickness $d_s = 2000$ Å with d_N varying between 75 and 400 Å. This set of curves is similar to conductance curves of BCS materials of various energy gaps. This point will be seen later with the discussion of Fig. 6. Let us note that the observation of a true energy gap in clean proximity system[22] is due to the directional selectivity of the tunneling. In a clean case, very low-energy excitations exist, which propagate parallel to the NS interface.[23] We follow Adkins and Kington[24] for the determination of the energy gap $\Delta_0(T)$ in Cu-Pb systems. For a given temperature T, we measure $\sigma(0, T)$. We choose $\Delta_0(T)$ as the value which would give the same $\sigma(0, T)$ on a BCS superconductor.

$\Delta_0(T)$ is represented Fig. 5(a). At high temperatures, we observe an increase of $\Delta_0(T)$, when T decreases, typical of a BCS superconductor. At low temperatures, this determination gives decreasing values for $\Delta_0(T)$ which arise from the nontunneling part of the junction conductance. The maximum value of $\Delta_0(T)$ is taken as Δ_0. We call the BCS superconductor of gap Δ_0 the equivalent BCS (EBCS). We also introduce the EBCS criti-

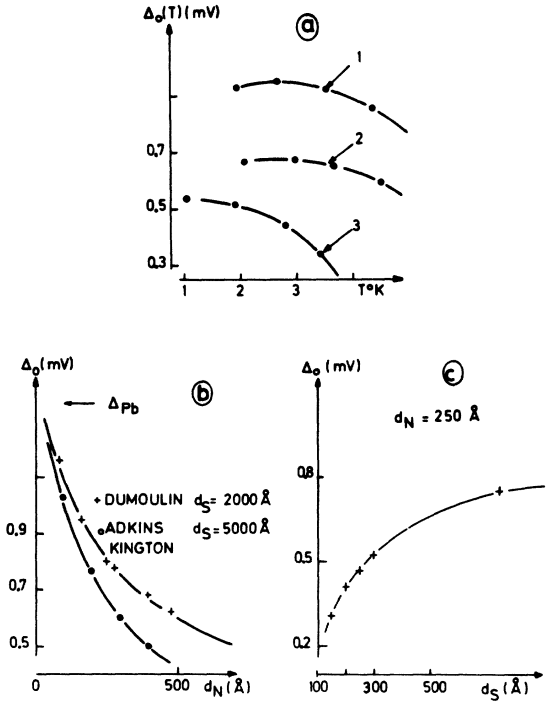

FIG. 5. Energy gap in Cu-Pb measured from the value of the BCS conductance at zero bias: (a) vs temperature for (1) Cu (150 Å)/Pb(2000 Å), (2) Cu(280 Å)/Pb(2000 Å), (3) Cu(250 Å)/Pb (300 Å); (b) vs Cu film thickness d_N for a large Pb film thickness d_S; (c) vs d_S at a given d_N.

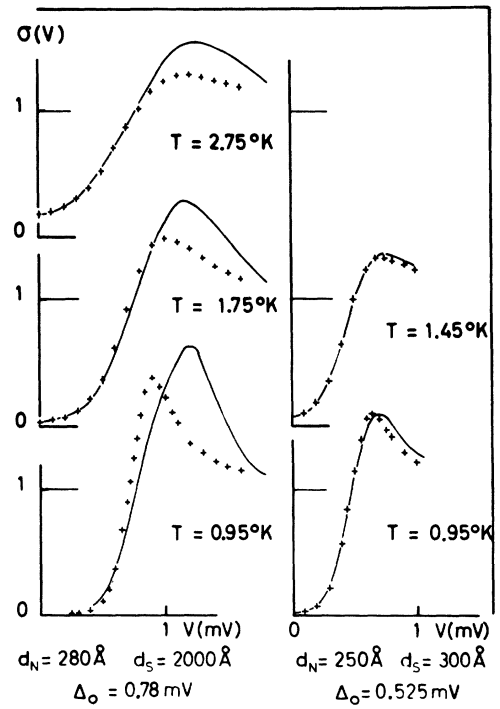

FIG. 6. Comparison at different temperatures between the measured conductance (solid line) on Cu-Pb and the calculated BCS conductance (crosses). The agreement is excellent when both films are thin (Cooper limit).

cal temperature $T_c^* = \Delta_0/1.76k_B$.

Figure 6 gives a comparison of the conductance curves $\sigma(V,T)$ measured on Cu-Pb and calculated for the EBCS. We distinguish two cases: (i) $d_s \gg \xi_s$ (the coherence length on Pb ~ 800 Å). The EBCS describes well the observed density of states at energies lower than Δ_0. At higher energies, in Cu-Pb, the BCS singularity at Δ_0 is replaced by a broad maximum, whose location is reminiscent of the Pb energy gap. (ii) $d_s \ll \xi_s$. The EBCS describes well the conductance observed on Cu-Pb at all energies.

The MacMillan model for the proximity effect[21,3] gives an excellent account of the above results. Qualitatively, when both films are very thin compared with their coherence lengths (Cooper limit), a BCS-like behavior is expected with an effective interaction parameter[25]

$$(NV)_{eff} = (N_N^2 V_N d_N + N_s^2 V_s d_s)/(N_N d_N + N_s d_s) .$$

Figures 5(b) and 5(c) gives our Δ_0 results versus d_N and d_s. We find values larger than those of Adkins and Kington's because we have a larger transmission coefficient between N and S as already discussed in Ref. 3.

E. Conclusion

Superconductivity induced by proximity is uniform across the thickness of thin and clean Cu films. The density of states is close—notably in the low-energy range considered in the following—to that of a BCS superconductor with a gap Δ_0 and a critical temperature T_c^*. When magnetic impurities X are introduced in Cu, their interaction with conduction electrons is not perturbed, in the normal state, by the proximity effect and remains characterized by the value T_K for the CuX alloy film alone. In the superconducting state, we compare our tunneling density of states with predictions done for an homogeneous alloy of Kondo temperature T_K and BCS matrix of critical temperature T_c^*.

IV. STUDY OF THE *Cu*Cr-Pb SYSTEM

Here we discuss in detail the effect of: temperature (Sec. IV A); impurity concentration (Sec. IV B); and T_K/T_c (Sec. IV C). *Cu*Cr was chosen because the T_K value ~ 1K is of the order of magnitude of accessible T_c^*. Our results are compared with the ZBMH calculation (see Sec. III C)

at the end of each section and discussed in detail in Sec. IV D.

A. Temperature dependence

1. Experimental results

Figure 7(a) gives the tunneling conductance at different temperature T for one *Cu*Cr-Pb sandwich having the following parameters: $d_N = 250$ Å, $c = 17$ ppm, $d_s = 2000$ Å, $\Delta_0 = 0.8$ mV, and $T_c^* = 5.3$ K. We can distinguish three domains of T:

(i) Low temperature ($T < 0.8$ K in this experiment). The presence of a localized impurity band within the gap is clearly shown by a maximum of conductance σ_m at an energy which is weakly temperature dependent (5% decrease between 0.4 and 0.8 K).

(ii) Intermediate domain ($0.8 < T < 1.3$ K). An inflexion point (σ_I, y_I) is seen on the conductance curve. The energy y_I can be determined accurately using a second-derivative technique. We see that $y_I = y_m \pm 10\%$.

(iii) High temperature ($T > 1.3$ K). No anomalous structure is observed. However, the conductance at low energy is large. Its shape and amplitude disagree strongly with the KZ model based on the AG picture (even if we take an enhanced value Γ_{eff} for Γ, as was done in our previous work[3]).

2. Comparison with the ZBMH calculation

Fig. 7(b) shows the ZBHM density of states computed with $y_0 = 0.34$, $\Delta = \Delta_0 = 0.8$ mV, $c = 17$ ppm. The value of y_0, discussed later in Sec. IV D, has been adjusted to reproduce the experimental location of the conductance maximum at the lowest temperature [Fig. 7(a)]. It is the only adjusted parameter. The value Δ_0 has been taken from Cu-Pb sandwiches having the same geometrical parameters (see Sec. IV D). We take $\Delta = \Delta_0$ because, at very low concentrations, the renormalization of the order parameter is negligible. The concentration c is obtained from the slope of the logarithmic dependence of the resistivity at low temperature on a test film prepared at the same time as the junction.[3] We also give in Fig. 7(b) the tunneling conductance computed at finite temperature using formula (1). The comparison of Figs. 7(a) and 7(b) leads to the following remarks:

(i) The experimental shape and height of the band agree with calculation.

(ii) The degradation of the resolution as T increases is explained well by the thermal smearing effect alone. There is no need to introduce any temperature dependent shape for the impurity band (see Sec. III C) in the low-temperature range (when Δ_0 does not vary any more with T).

(iii) In order to characterize any discrepancy between experiment and theory in the height of the band, we calculate theoretically a conductance curve and take the inverse ratio K of its conductance peak to that observed experimentally at the same temperature. We find this ratio to be temperature independent (within 5%). In this experiment $K \simeq 1.25$. This value will be discussed in Sec. IV C4.

B. Impurity concentration study

1. Experimental results

We present a series of experiments on *Cu*Cr-Pb sandwiches: c varies from 25 to 300 ppm. The

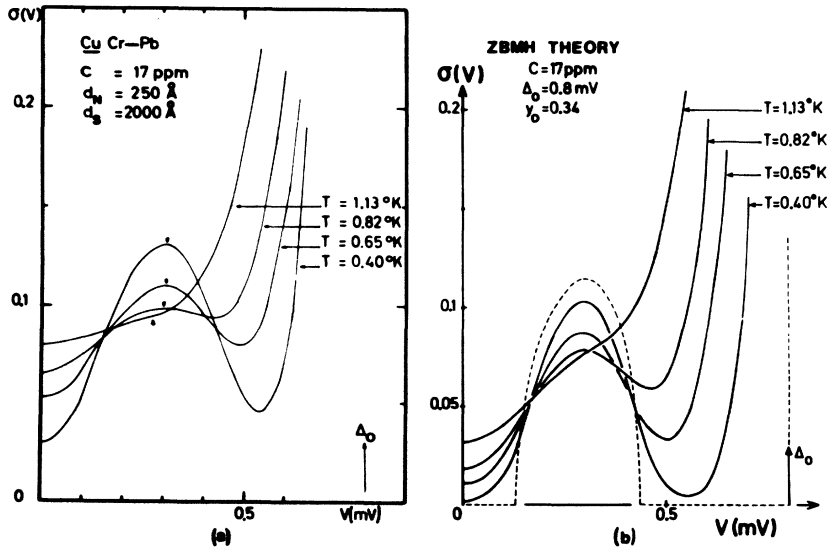

FIG. 7. (a) Experimental tunneling conductance vs bias. At the lowest temperature, the impurity band is well resolved. The thermal smearing washes out this structure at high temperature. (b) Theoretical density of states (dotted line) computed with the parameters of the experiment reported in Fig. 7(a). y_0 was adjusted to give account for the experimental location of the band. The solid lines give the conductance calculated for various temperatures.

geometrical parameters $d_N = 250$ Å, $d_s = 2000$ Å were kept as constant as possible through the samples: thus Δ_0 and T_c^* are constant. The Fig. 8 gives the general results at 0.95 °K, while Fig. 9 describes in greater detail the density of states within the "gap." The thermal smearing is important at 0.95 K. However, with concentrations larger than 25 ppm, we are still in the low temperature domain, defined in the previous paragraph, in which a maximum of conductance can be observed. Then, y_m is a good indication of the energy location of the top of the band and σ_m an indication (within 25%) of its height.

2. *Analysis of the results and comparison with theory*

When the concentration increases the following result:

(i) σ_m increases. The inset in Fig. 8 shows that σ_m varies as $\sqrt{c}$. This agrees with theory as one can see from formula (3), valid in the low concentration limit.

(ii) y_m moves slightly towards the high energies. The exact calculation accounts for this fact: starting at low concentration with a parabolic shape centered around $y_0\Delta$ [formula (3)] the band develops asymmetrically, its maximum moving towards higher energies [see Fig. 3(b)].

(iii) The conductance peak at y_m becomes less marked and finally disappears. However, the low-energy conductance remains remarkably large and flat as compared with AG predictions. For increasing concentration, the theory predicts that the band also widens, touches the gap edge and finally gives a flat continuum inside the initial gap [see Fig. 3(c)]

(iv) The fast increase of the conductance near Δ_0 is still observed. We call this region "edge of the gap." Its characteristic energy $V_1[\sigma(V_1) = 1]$ moves towards large energies. In the KZ model[20] based on the AG picture, an opposite variation of V_1 towards low energies would be expected.

(v) The "singularity" above Δ_0 is softened. If we compare with the Cu-Pb case, it appears

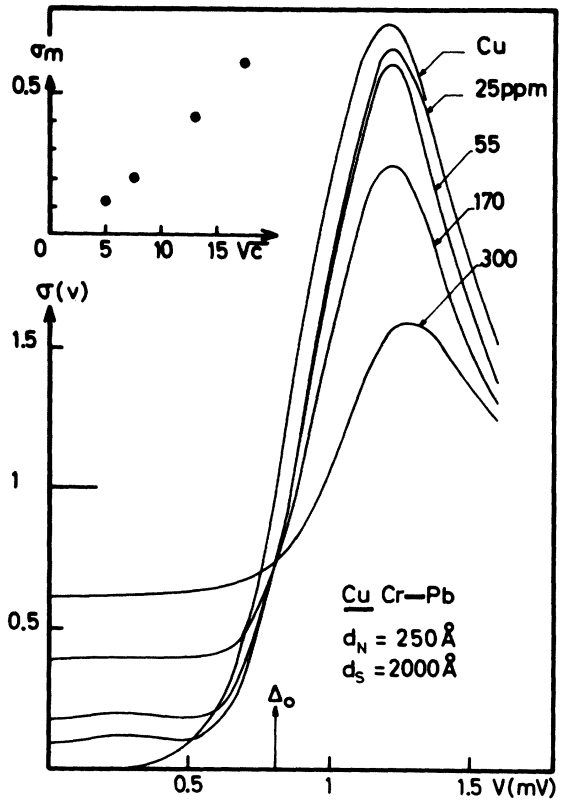

FIG. 8. Conductance curves obtained at 0.96 °K on sandwiches of identical geometry (identical Δ_0 and T_c^*) for different Cr concentrations. The edge of the "gap" shifts towards the high energies and the band develops as c increases. The inset shows that the height of the impurity band (σ_m) varies as $\sqrt{c}$.

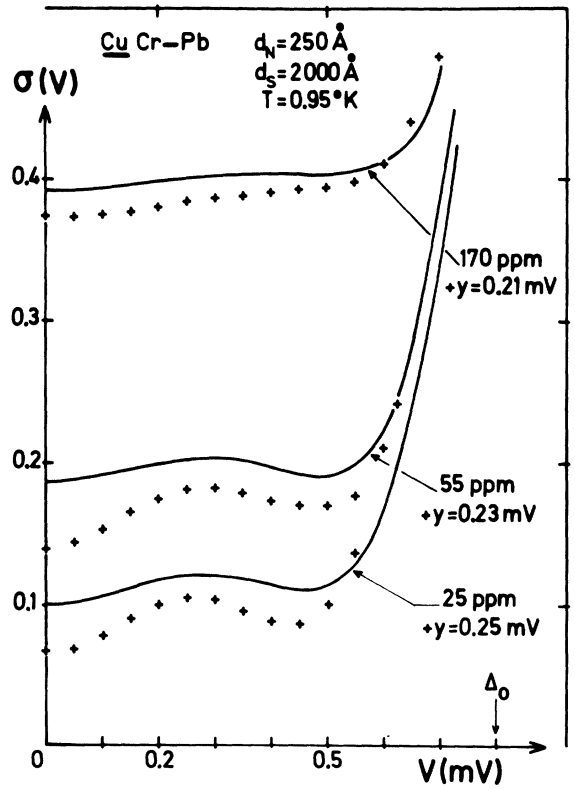

FIG. 9. Details of the conductance curves of Fig. 8 within the energy gap. Crosses give theoretical conductance. Calculation is made by adjusting only the location of the LES $y = y_0\Delta$; y_0 is constant and the variation of y is qualitatively accounted by that of $\Delta(c) < \Delta_0$ (renormalization of the order parameter).

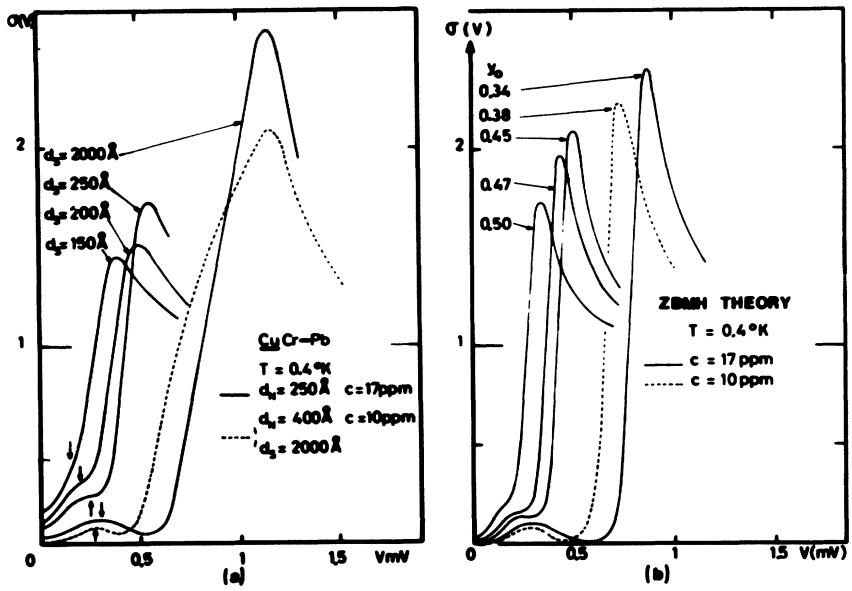

FIG. 10. (a) Solid lines give the tunneling conductance for four sandwiches made with identical *Cu*Cr films and Pb films of different thicknesses. Thus, we vary the induced energy gap in *Cu*Cr and study the effect of T_K/T_c^* for the same alloy. (b) Theoretical conductances associated with the experimental curves (a)–y_0 is adjusted for each curve in order to carry out its experimental variation with T_K/T_c.

qualitatively that the area lost below the curve at high energy is still recovered in the low-energy states. The agreement between experiment and theory on the first three points is illustrated quantitatively in Fig. 9.

The last two points are difficult to analyze quantitatively: near the gap edge, the conductance depends crucially on the renormalization of Δ, not calculated yet. In addition, the quasi-BCS approximation is poor above and around the energy-gap edge. We can, however, indicate a qualitative agreement with theory in which: (a) The edge of the continuum moves towards high energy in Δ units when c increases. This is opposite to the AG result where the gap ω_g decreases faster than the order parameter Δ. (b) The singularity above Δ is softened. The states which appear in the gap are taken from the gap edge [see formula (2)].

C. Effect of the variation of T_c^*

The proximity offers a means to vary independently the superconducting critical temperature on the same Kondo alloy. This is done by adjusting d_N and d_s (see Sec. III D).

(a) Large T_c^* values ($7 > T_c^* > 4.5$ K) are produced by covering with the same *thick* Pb film (2000 Å) several thin *Cu*Cr films of variable thickness (75–400 Å). For these values [see Fig. 2(b)] the localized states can be resolved in experiments at 0.95 K.

(b) Low T_c^* values ($4.5 > T_c^* > 2$ K) are obtained by coating several *Cu*Cr films of the same thickness $d_N = 250$ Å and obtained in the same evaporation with *thin* Pb films of different thicknesses (150–250 Å). The sample were studied at 0.4 K as the structures are not resolved as well as with high T_c^*. Typical conductance results are shown on Fig. 10(a).

Case (b) provides the best way to vary T_K/T_c^*, as the same alloy film is used in the experiments. Moreover, the use of thin Pb films is a good limit for the validity of a BCS approximation (see Sec. III D).

1. The location of LES

The energy location of the maximum or of the inflection in the conductance curves, provides good estimates of the LES position (see Sec. IV A). The values, reported in Table I, show a shift of the LES towards the edge of the continuum when T_c^* decreases.

As seen on Fig. 10(a), there is no inflection point on the conductance curve relative to the

TABLE I. Summary of localized-states data on *Cu*Cr-Pb. The energy location of the LES measured from the maximum (y_m) or point of inflection (y_I) of the conductance is given as a function of the gap $\Delta_0 = 1.76 k_B T_c^*$. We give also y_0 from the best fit with theory $y_0 \simeq y_m$ (or y_I)/Δ_0 and c, the concentration used for the experiment.

Δ_0 (mV)	1.2	1.0	0.8	0.69	0.46	0.4	0.3
T_c^* (°K)	(7.9)	6.25	5.3	4.5	3.0	2.6	2.0
y_m *ou* y_I	0.30	0.31	0.30	0.28	0.24	0.20	0.15
y_0 (expt.)	0.24	0.3	0.34	0.38	0.45	0.47	0.50
C (ppm)	10	10	17	10	17	17	17

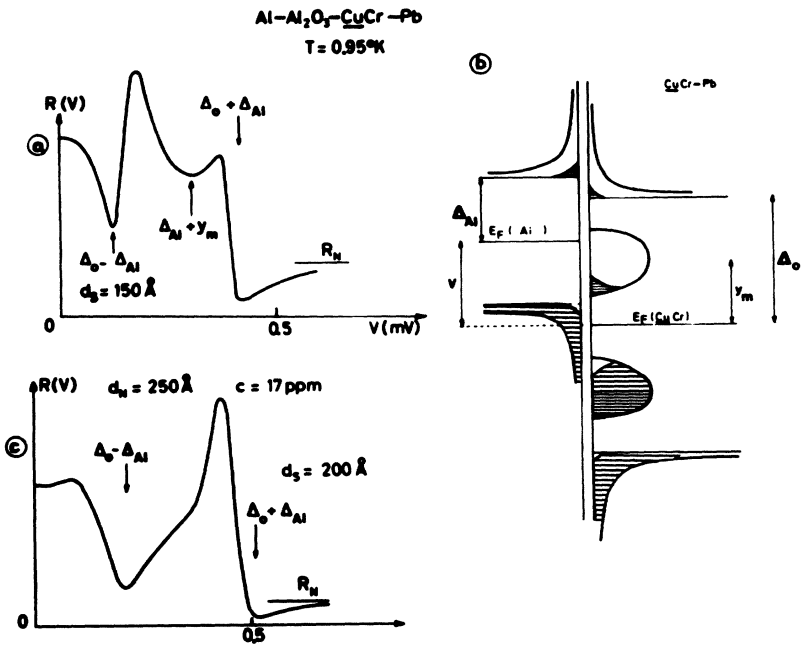

FIG. 11. Sandwiches identical to those of Fig. 10 are studied with a superconducting Al first electrode. The location of the gap and of the localized states in case of (a) can be done using the semiconductor diagram (b). In other cases (c) a deconvolution is needed due to thermal smearing.

sample having the lowest T_c^* ($d_s = 150$ Å). The thermal smearing (related to the value Δ_0/K_BT) is still too large at 0.4 K. In this case, the value y_m has been obtained using a first superconducting Al electrode of gap Δ_{Al} on an identical sandwich. Figure 11 shows experimental results. When $2\Delta_{Al} + y_m > \Delta_0$ [case of Fig. 11(a)] the evaluation of the LES position is straightforward as seen from the semiconductor diagram [Fig. 11(b)]. In the other cases [Fig. 11(c)] a deconvolution program is needed.[26] In both cases, the location of the LES agrees with the determination using a normal first electrode.

2. *Height of the band*

In the theory, the height h of the band is an increasing function of $\bar{c} = c/(2\pi N_0 \Delta)$ (see Sec. IIIC); h is proportional to $\sqrt{\bar{c}}$ at low concentration. In Fig. 10(a), we see that, keeping the concentration constant, the amplitude of the band (characterized by σ_m or σ_I) increases as Δ decreases.

3. *Quantitative analysis of the above results*

For each sandwich studied at a temperature T, we calculate the ZBMH density of states and the corresponding tunneling conductance at T. We proceed as in Sec. IVA2; c is given by the resistivity of a test alloy film, Δ_0 is the tunneling gap of a Cu-Pb sandwich of identical geometry, and y_0 is adjusted to get the correct maximum or inflexion of the experimental curve. The values of y_0 are given Table I and plotted Fig. 12(c). A

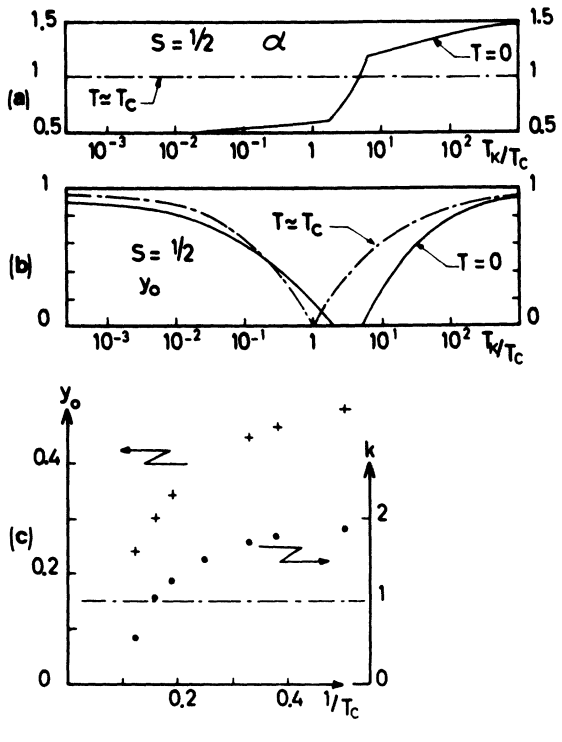

FIG. 12. (a) and (b) Theoretical dependence (from Ref. 2) of the spectral weight α and location of the LES, y_0, in the $T \to T_c$ limit (half-broken line) and $T = 0$ limit (solid line). (c) Experimental results on *Cu*Cr-Pb. K is obtained from the band height and related to α (see text).

good agreement is found between the theoretical conductance curves [Fig. 10(b)] and the experiments of Fig. 10(a).

The ratio $K=\sigma_m$ (or σ_I) experimental/σ_m (or σ_I) theoretical (Sec. IV A2) increases as T_c^* decreases [see Fig. 12(c)].

4. *Interpretation of the dependence of K with T_c^**

Until now, we have used the ZBMH calculation ($T \to T_c$ limit). However, our experiments are closer to the $T=0$ limit (see Sec. III C). The height of the band at finite concentration at $T=0$ is a complex (uncalculated at present time) but certainly increasing function of the spectral weight (density of states brought by one impurity alone). In the $T \to T_c$ limit, $\alpha=1$. In the $T=0$ limit, α depends on T_K/T_c^* [see Fig. 12(a)]. The variation of K with T_K/T_c^* is thus connected to the expected variation of α.

D. Discussion

Throughout this chapter we have compared our results with theory using adjusted values of the location y_0 of the LES. We compare now the y_0 values with theoretical predictions [see Sec. III C and Fig. 12(b)].

The experiments described in A and B correspond to $T_c^*=5.3$ K and an adjusted value $y_0=0.34$. It is currently agreed that the T_K of CuCr is about 1 K. For this value of the ratio T_K/T_c^*, the theoretical estimate is $y_0=0.27$, in agreement with the experimental determination (Ref. 4). However, the variation of y_0 with T_K/T_c^* (if $T_K=1$ K) observed in Sec. IV C [Fig. 12(c)] is opposite from the predicted one [Fig. 12(b)]. A comparison of these two figures shows that the CuCr experiments should correspond to $T_K > T_c$. This result is also obtained from a comparison of K [Fig. 12(c)] and α [Fig. 12(a)] variation with T_K/T_c. Our results would be well described with a large value $T_K \simeq 20$ K.

We do not think that T_K in our films should be strongly different from the bulk[28] $T_K \simeq 1$ K; the low-temperature resistivity of films agrees with bulk results (3). Figure 13 also gives negative magnetoresistance measurements on a CuCr film (compared to measurements on bulk[27]) $\Delta\rho_i(T,H) = \rho_i(T,H=0) - \rho_i(T,H)$. The positive magnetoresistance of a pure Cu film of same thickness is negligible because the electronic mean free path is strongly reduced by surfaces. In a first approximation $[\rho_i(T)/\Delta\rho_i(T,H)]^{1/2}$ is proportional[27] to χ^{-1}, where χ is the magnetic susceptibility of impurities. We find a Curie-Weiss law between 1 and 4 K. The intercept of the straight line, $\chi^{-1}(T)$, with the T axis gives the order of magnitude of $^{28}T_K$: we see again that T_K values in CuCr films much larger than 1 K are excluded.

We conclude that the theory gives the main features of the impurity band phenomenon but fails to predict its exact location in the CuCr-Pb case. We will come back to this point in the conclusion, after a comparative study of alloys of different T_K.

V. IMPURITY BANDS STUDY IN OTHER SYSTEMS

A. *Au*Fe-Pb system

A T_K value of about[28] 0.5 K is generally accepted for dilute AuFe alloys. The Au-Pb sample is metallurgically poor for proximity effect. In order to avoid the interdiffusion and formation[14] of

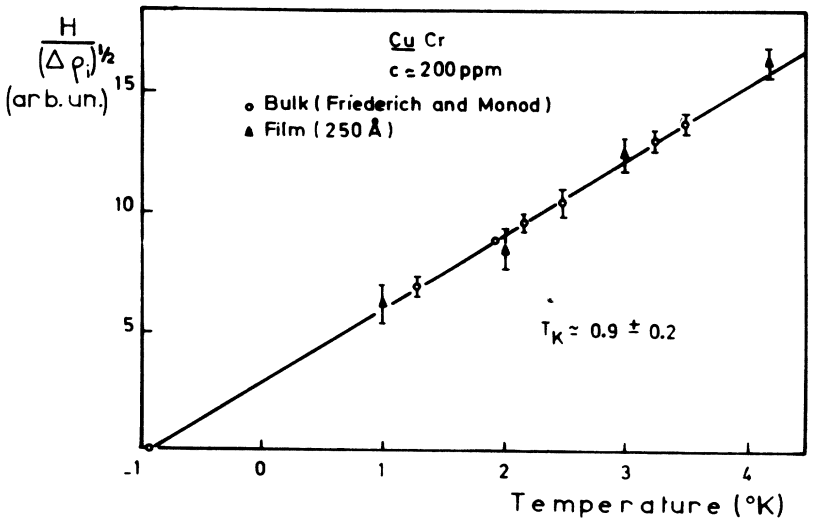

FIG. 13. Negative magnetoresistance $\Delta\rho_i$ of a CuCr. The results show a Curie-Weiss behavior and lead to a T_K value near 1 K for bulk and films. (We thank A. Freiderich and P. Monod for the use of their results before publication.)

$AuPb_2$ and $AuPb_3$ it is necessary to maintain the sample at low temperatures.

1. Experimental procedure

The *Au*Fe films are evaporated at room temperature. Then substrates are cooled down to −100 °C and the alloy film is covered by the Pb film. The samples remain in contact with a cooling source up to the time where the sample is put in the precooled helium cryostat. We estimate that the samples remain at most one to two minutes at a highest temperature of −50 °C.

2. Quality of samples versus tunneling results

The normal side tunneling conductances measured at 0.95 K with a first normal electrode are shown in full line on Fig. 14. The curves have a point of inflection within the gap. At higher energy, they are very similar to those of Cu-Pb of the same geometry. We can use the same analysis;

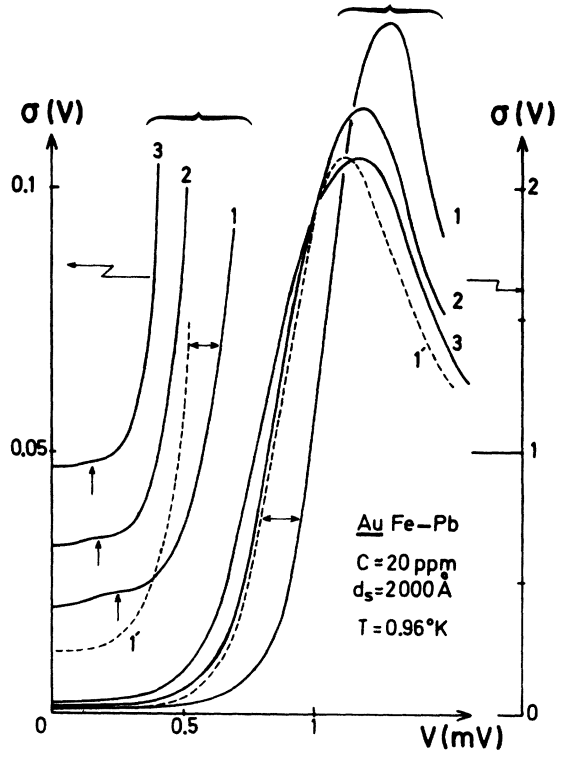

FIG. 14. Tunneling conductance of three *Au* Fe-Pb sandwiches kept at low temperature before study (solid lines). The arrows give the exact location of the point of inflection obtained from second derivative (d^2I/dV^2). The dotted line (curves 1′) was obtained on sandwich (1) after 2 h at room temperature: the interdiffusion had reduced the gap and put out the band structure. (1) d_N = 150 Å; (2) d_N 250 Å; (3) d_N 325 Å. Note the different conductance scales on the two sets of corresponding curves.

in particular Δ_0 is well given by V_1. On Fig. 14, we have plotted in dotted line the tunneling conductance of one Au-Fe-Pb sandwich after a 2-h storage at room temperature. The gap is strongly reduced and the structure at low energy has disappeared. We can assume that diffusion in *Au*Fe has reduced the electronic mean free path (lowering the gap next to the barrier) and has changed the magnetic properties of the alloy (disappearance of the impurity band).

3. Analysis of the impurity band

In this experiment, the concentration, determined by the logarithmic slope of the low-temperature resistivity of test *Au*Fe films, is about 10 ppm of Fe. The resolution of the impurity band is poor. We are in the intermediate domain of experimental temperatures (see Sec. IV A1): the band is revealed only by a point of inflection on the conductance curve which gives the location of the LES (within 10% accuracy) and the height of the band (within 30% accuracy). Another experiment[29] with 20 ppm of Fe in Au is consistent with a height varying as $\sqrt{c}$. Results on the location of the LES y_0 vs T_K/T_c are given in Table II. The shift of y_0 with T_K/T_c agrees with theory. The experimental results would be exactly described if T_K was 1.25 K instead of 0.5 K for the bulk; this is a rather good agreement.

Very recently, Claeson has reported[30] a value $y_0 \simeq 0.6$ for *Au*Fe-Pb of estimated concentration 100 ppm. We suggest that the larger y_0 value could be due to a decrease of the "effective Kondo temperature" of the alloy when the concentration increases (interaction effect between impurities).[31]

The *Au*Fe-Pb system appears very interesting in order to study a LES crossing the center of the gap (it is easy to get $T_c^* \sim T_K$) and the appearance of interactions effects at increasing concentration.

More detailed and systematic experiments are clearly needed. Results using *in situ* measurements in a cryogenic evaporation are in progress.

TABLE II. LES location for *Au* Fe-Pb experiments (presented as in Table I). The impurity concentration is 10 ppm. We give the theoretical predictions for two different values of T_K.

Δ_0 (mV)	0.980	0.820	0.775
T_c^* (°K)	6.45	5.40	5.1
y (mV)	0.25	0.175	0.145
y_0 (expt.)	0.25	0.21	0.19
y_0 (theory) $T_K = 0.5$ °K	0.38	0.36	0.35
y_0 (theory) $T_K = 1.25$ °K	0.25	0.23	0.22

B. Study of the *Cu*Mn-Pb system

The T_K value of *Cu*Mn (≃0.01 K) is much smaller than T_c^* values. We have studied *Cu*Mn-Pb sandwiches at 0.4 K with different thicknesses but the same concentration (between 10 and 20 ppm) of the alloy film. The tunneling conductance curves are shown Fig. 15. From the location of the inflection point , we get a value $y_0 \simeq 0.6$ in excellent agreement with theory (see also Table III).

1. Remark

On Fig. 15, the dashed lines reveal some anomalies in the curves. The deviation is more clearly seen when Δ_0/K_BT increases and the resolution improves. The first one at 0.3 mV could be interpreted by the presence of 0.1 ppm of Cr. The other one, near 0.8 mV, is only visible on sample 1 of larger gap and could be due to uncontrolled Fe (≃1 ppm) impurities (see Secs. IV C and IV D).

2. Effect of the concentration

We have studied, at 0.96 K, alloys of two concentrations 50 and 500 ppm, with the same set of geometrical parameters indicated on Fig. 16. Dashed lines give the ZBMH density of states calculated using the theoretical value for the location of the LES: $y_0 = 0.64$. In the 500-ppm case, the band is no longer localized in energy and merges with the continuum. The corresponding calculated conductance at $T = 0.96$ K agrees well with the experimental results. However, the ratio K introduced above (Sec. IV A) is smaller than 1. This is an agreement with the fact that α is smaller than 1 (in the limit $T = 0$) when $T_K \ll T_c$ [see Fig. 12(a)].

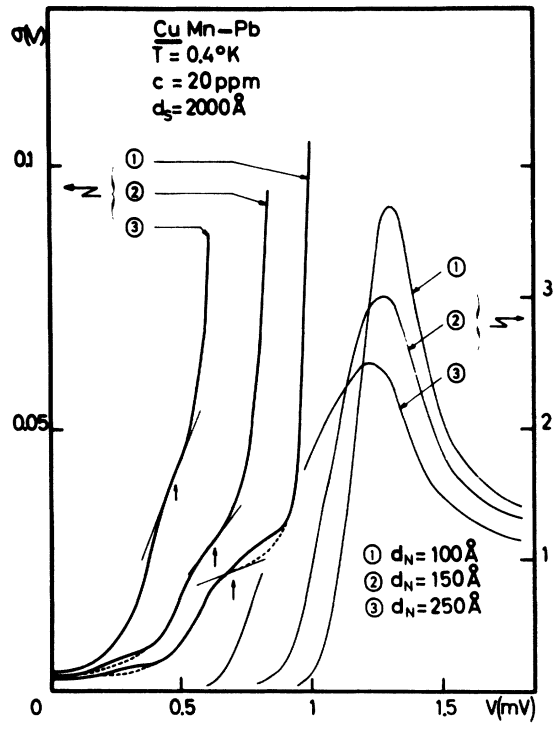

FIG. 15. Tunneling conductance on very dilute (< 20 ppm) *Cu*Mn-Pb sandwiches. The additional structures around 0.3 and 0.8 mV could be due to very dilute uncontrolled impurities (see text).

TABLE III. LES for *Cu*Mn-Pb experiments (presented as in Table I). Note the good agreement with theory for $T_K \ll T_c^*$.

Δ_0 (mV)	1.1	1.0	0.81
T_c^* (°K)	7.3	6.6	5.4
y_I (mV)	0.7	0.63	0.48
y_0 (expt.)	0.63	0.63	0.59
y_0 (theory)	0.65	0.64	0.63
T_K = 0.01°K			

C. Study of the *Cu*Fe-Pb system

Here T_K(≃30 K) is larger than T_c^*. We have studied *Cu*Fe-Pb sandwiches for a wide range of parameters (d_N, d_S, and c) corresponding to those used for the previous alloys.

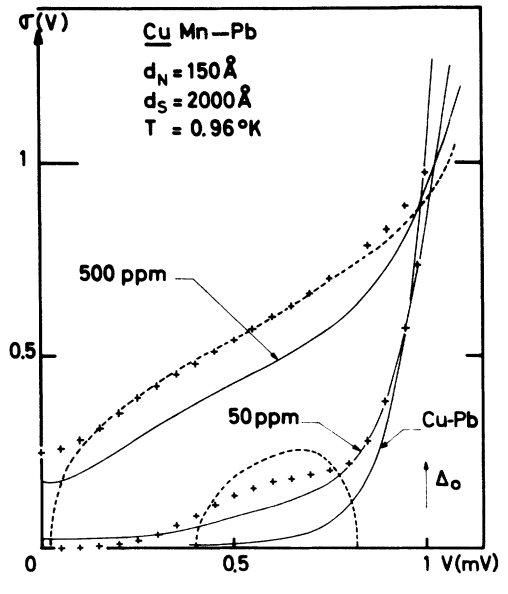

FIG. 16. Concentration effect on *Cu*Mn-Pb. Solid lines: experimental conductance. Crosses: theoretical conductance without any adjustable parameter. Dotted lines: theoretical density of states. Note that, at high concentration, the band merges into the continuum.

1. Location of the band in CuFe-Pb system (Ref. 32)

Figure 17 gives the tunneling conductance obtained at 0.07 K on a 10-ppm *Cu*Fe film backed by Pb (the first *Al*Mn electrode is normal). A LES is clearly obtained here and its location, given by $y_0 = 0.85$, is very close to the gap edge. We have studied a series of sandwiches differing only by the normal film thickness, $d_N = 75-500$ Å (Δ_0 varies from 1.2 to 0.6 mV). When the gap decreases—that is to say when T_K/T_c^* increases—the LES moves towards the gap edge (y_0 increases). The band is not longer resolved, even at 70 mK, when Δ_0 becomes smaller than 0.8 meV. This illustrates the difficulties in resolving the band when it is close to the gap edge. The two mechanisms giving a loss of resolution when decreasing Δ_0 for a given concentration are: (i) the thermal smearing acting roughly as $k_B T/\Delta_0$; (ii) the size of the band, related to $\bar{c} = c/(2\pi N_0 \Delta)$ (Sec. III C): the band merges into the continuum when $\bar{c}$ increases.

2. Comparison with theory

The shift of the LES with T_K/T_c^* agrees with the theoretical prediction in the situation $T_K > T_c$. The size of the band agrees well with a spectral weight of one state by impurity. However, its location disagrees strongly with theory: we find $y_0 = 0.85$ instead of 0.34 as predicted.

3. Concentration effect

Figure 18 gives a concentration study on *Cu*Fe/Pb at $T = 0.96$ K similar to that made on *Cu*Cr/Pb and reported Fig. 8. The experimental temperature is too high to follow the shape of the band. (It is no longer possible to observe the LES very close to the gap even when using a superconducting first electrode). However, we can make the two remarks:

(a) The impurity spin S and $(\ln T_K/T_c)^2$ are the same for *Cu*Cr/Pb and *Cu*Fe/Pb in the two series of experiments and theory predicts the same results (Sec. III C). This theoretical prediction is in disagreement with experiments.

(b) The set of curves of Fig. 18 is reminiscent of an AG shape which would correspond to $T_K/T_c \to 0$. In fact, we are in the opposite limit! This remark leads to a word of warning when interpreting tunneling conductance results carried on high-concentration alloys and high-T experiments if one wants to deduce T_K values from the conductance shape.

D. On some possibilities of the tunneling study of Kondo superconducting systems

Figure 19 gives the tunneling conductance obtained at 70 mK on a Cu-Pb sandwich. The pure[33] Cu and contains nominally mostly 0.5 ppm of Fe as residual impurities. We find two peaks in the density of states within the gap. They can be illustrated at 2.10^{-2} ppm of Cr (0.34-mV peak) and

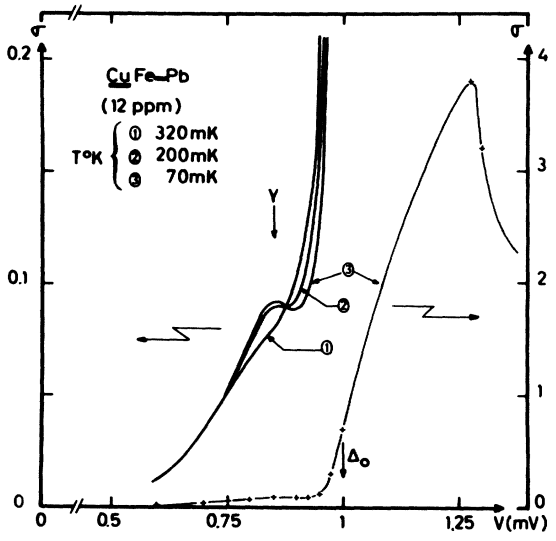

FIG. 17. Tunneling conductance on *Cu*Fe-Pb sandwiches ($d_N = 150$Å, $d_S = 2000$ Å) at very low temperature.

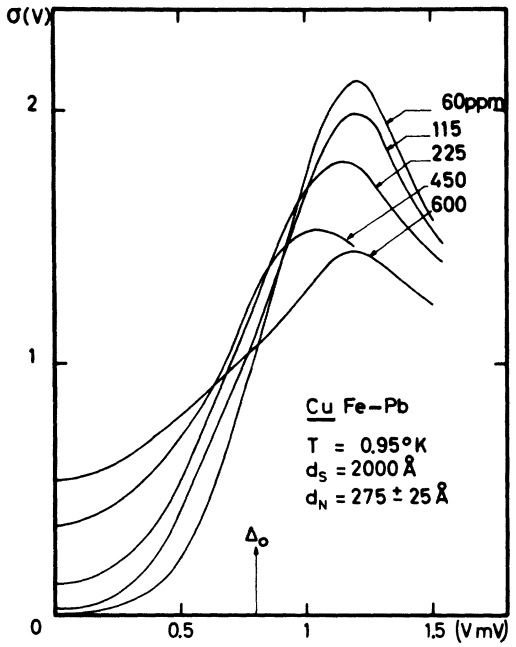

FIG. 18. Concentration effect on *Cu* Fe-Pb at 0.96 °K. The band does not appear except possibly on the most concentrated alloy. A depression of the gap is obtained with gapless when c increases.

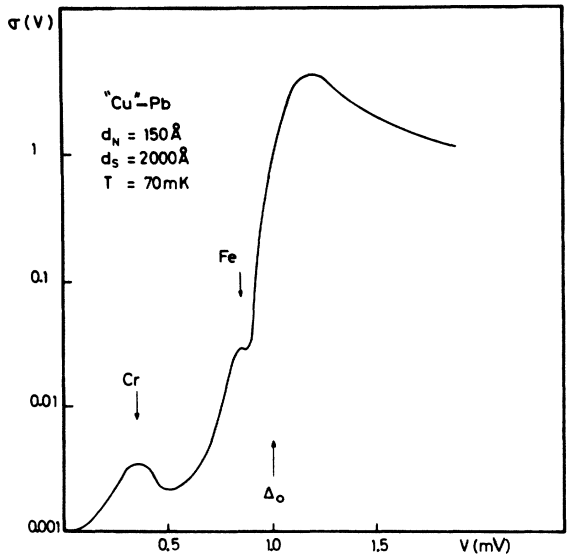

FIG. 19. Tunneling conductance observed at very low temperature on Cu-Pb sandwich. The "pure" Cu film contains 0.02 ppm of Cr and 1 ppm of Fe as estimated from the size of the impurity bands observed at 0.34 and 0.85 meV.

1 ppm of Fe (0.85-mV peak). Possible contamination can arise from the Mo crucible used in the Cu evaporation. The result is consistant with the slow increase in the resistivity observed with decreasing temperature below 10 K on a test Cu film. This illustrates the sensitivity of the tunneling approach. Its spectroscopic character gives the appreciable advantage—compared to resistivity for instance—for discriminating the contribution of the impurity to be studied from those arising from unwanted very dilute impurities. Let us note, however, the need of very good tunneling junctions. Here, the nontunneling conductance is smaller than 10^{-3}.

VI. CONCLUSION

In Table IV, we have summarized our results concerning the location of the LES and have compared them with the theoretical results of Müller-Hartmann and Zittartz. The agreement is good for $T_K \ll T_c^*$. It deteriorates progressively as T_K becomes of the order and larger than T_c^*. This corresponds to the transition towards the low-temperature strong-coupling limit, where the perturbation theory is no longer valid. This degradation of agreement has also been observed on other properties of dilute magnetic alloys.[34]

Recently, an exact numerical solution of the Kondo problem, using renormalization-group technique, has led to determination of the complete

TABLE IV. The energy location of the LES for the alloys studied here. (When the equivalent BCS critical temperature T_c^* of the sandwich alloy-Pb is 5 °K.) The arrows indicate the sense of variation of y_0 if T_K/T_c^* increases. We find agreement with theory when $T_K \ll T_c^*$.

Alloy	T_K (°K)	y_0 (for $T_c^* = 5$ K) Expt.	Theory
Cu Mn	0.01	0.6 ↓	0.62 ↓
Au Fe	0.5	0.2 ↓	0.35 ↓
Cu Cr	1	0.34 ↑	0.27 ↓
Cu Fe	30	0.85 ↑	0.27 ↑

T dependence of resistivity and susceptibility of normal Kondo alloys.[35] However, a systematic study of the intermediate regime in normal alloys will not probably be very attractive to theoreticians or experimentalists: it requires very elaborate and difficult numerical techniques and on the other hand, gives only a simple interpolation between the well-known low-temperature and high-temperature regimes. This is not so in the superconducting case. The crucial regime turns out to be that where T_K and T_c and, consequently, the experimental temperatures of interest, are of the same order of magnitude. The solution of this "intermediate range" problem is probably very difficult. On the other hand, experiments like the tunneling ones reported here provide a very selective tool to approach it.

This study provides several points indicative of the variation of y_0 vs T_K/T_c^*, and a systematic study using the flexibility of the proximity in providing an independent T_c^* variation should be available soon. It is of great interest to evaluate the degree of universality of such a variation which should also include the effect of the value of the impurity spin S.

From such a curve, one could obtain directly the T_K value of very dilute alloys (in particular metastable alloys obtained by quench condensation). It is important to have several experiments with different T_c^* in order to discrimate between the $T_K \gtrless T_c^*$ behavior. The large sensitivity and spectroscopic character of the method is also of interest in the extreme dilution experiments where several residual species may be present together.

Finally, it is clear that the quantitative analysis rests heavily on the quasi-BCS approximation which has been extensively discussed in the context of our experiments. Despite the metallurgical difficulties in the obtention of homogeneous superconducting alloys, it would be highly desirable to have tunneling results on homogeneous systems.

ACKNOWLEDGMENTS

The authors express their gratitude to J. P. Burger, K. Maki, C. D. Mitescu, P. Monod, and E. Müller-Hartmann for interesting discussions, to A. Bringer for giving to us the program of band calculation, to G. Belessa and D. Le Fur for their help in the low-temperature experiments.

---

*Part of a thesis by L. Dumoulin, Université de Paris Sud (1975).

†Laboratoire associé au centre National de la Recherche Scientifique.

[1](a) General review: M. B. Maple (1973), in *Magnetism*, edited by H. Suhl (Academic, New York, 1975), Vol. 5, Chap. 10; (b) Works concerning especially the problem of states in the gap of Kondo superconductors: A. S. Edelstein, Phys. Rev. Lett. 19, 1184 (1967); Phys. Rev. 180, 505 (1969); H. V. Culbert and A. S. Edelstein, Solid State Commun. 8, 445 (1970); T. Sugawara and S. Takayanagi, in *Proceedings of the 14th International Conference on Low Temperature Physics*, edited by Matti-Krusius and Matti Vuorio (North-Holland/American Elsevier, Amsterdam, 1975); (c) E. Müller-Hartmann in *Magnetism*, edited by H. Suhl (Academic, New York, New York, 1973), Vol. 5, Chap. 10.

[2](a) General work on proximity effect: J. J. Hauser, H. C. Theurer, and N. R. Werthamer, Phys. Rev. 142, 118 (1966); T. Claeson, in *Tunneling Phenomena in Solids*, edited by E. Burstein and S. Lundqvist (Plenum, New York, 1969), Chap. 30; K. E. Gray, Phys. Rev. Lett. 28, 959 (1972); (b) Application to the study of magnetic alloys: T. W. Mikalisin, D. P. Snowden, and P. M. Chaikin, Bull. Am. Phys. Soc. 13 (1968); J. J. Hauser, D. R. Hamann, and G. W. Kammlott, Phys. Rev. B 3, 2211 (1971).

[3]L. Dumoulin, E. Guyon, and P. Nedellec, J. Phys. (Paris) 34, 1021 (1973).

[4]L. Dumoulin, E. Guyon, and P. Nedellec, Phys. Rev. Lett. 34, 264 (1975).

[5]A. A. Abrikosov and L. P. Gor'kov, Zh. Eksp. Teor. Fiz. 39, 1781 (1960) [Sov. Phys.-JETP 12, 1243 (1961)].

[6]M. A. Woolf and F. Reif, Phys. Rev. 137, A557 (1965).

[7]I. Giaever, in *Tunneling Phenomena in Solids*, edited by E. Burstein and S. Lundqvist (Plenum, New York, 1969), Chap. 3.

[8]D. E. Thomas, and J. M. Rowell, Rev. Sci. Instrum. 36, 1301 (1965); we used exactly the same device as P. Guetin and G. Schreder, J. Appl. Phys. 43, 549 (1972).

[9]We have given a systematic study of these structures for Cu film thickness in the range 1000–3000 Å, taking into account phonon renormalization and geometrical resonances, in P. Nedellec, L. Dumoulin, and E. Guyon, Solid State Commun. 9, 2013 (1971).

[10]A. Leger, thesis (Paris, 1971) (unpublished). A. Gilabert, J. P. Romagnan, and E. Guyon, Solid State Commun. 9, 1295 (1971).

[11]J. M. Rowell, See Ref. 7, Chap. 27.

[12]E. L. Wolf, in *Solid State Physics*, edited by H. Ehrenreich, F. Seitz, and D. Turnbull (Academic, New York, 1975), Vol. 30, p. 2.

[13]G. I. Rochlin, L. Dumoulin, and E. Guyon, Solid State Commun. 8, 287 (1970).

[14]A. F. Hebard, J. Vac. Sci. Technol. 10, 606 (1973).

[15]M. Fowler and K. Maki, Phys. Rev. B 1, 181 (1970).

[16]S. Skalski, O. Betbeder-Matibet, and P. R. Weiss, Phys. Rev. 136, A1500 (1964).

[17]H. Shiba, Prog. Theor. Phys. 40, 435 (1968).

[18]H. Shiba, Prog. Theor. Phys. 50, 50 (1973).

[19]J. Zittartz, A. Bringer, and E. Muller-Hartmann, Solid State Commun. 10, 513 (1972).

[20]A. B. Kaiser and M. J. Zuckermann, Phys. Rev. B 1, 229 (1970).

[21]W. L. McMillan, Phys. Rev. 175, 537 (1969).

[22]S. M. Freake and C. J. Adkins, Phys. Lett. 29, A382 (1969).

[23]P. G. De Gennes, and D. Saint-James, Phys. Lett. 4, 151 (1963).

[24]C. J. Adkins and B. M. Kington, Phys. Rev. 177, 777 (1969).

[25]G. Deutscher and P. G. De Gennes, in *Superconductivity*, edited by R. D. Parks (Dekker, New York, 1969), Vol. 2, p. 1005.

[26]A. Gilabert, thesis (Nice, 1975) (unpublished); and private communication.

[27]A. Friederich, Thèse de 3ème cycle (Orsay, 1972) (unpublished); and to be published; M. D. Daybell and W. A. Steyert, Phys. Rev. Lett. 20, 195 (1968).

[28]M. D. Daybell, in *Magnetism*, edited by H. Suhl (Academic, New York, 1973), Vol. 5, Chap. 4.

[29]This experiment was made with Dr. Claeson during a CNRS mission in Orsay, We want to thank him for his help and useful discussions.

[30]T. Claeson, in *Proceedings of the 14th International Conference on Low Temperature Physics*, edited by Matti-Krusius and Matti-Vuorio (North-Holland, Amsterdam, 1975), Vol. 3, p. 448.

[31]J. L. Tholence, thesis (Grenoble, 1973) (unpublished).

[32]L. Dumoulin and D. Le Fur, C. R. Acad. Sci. Paris 282, B 193 (1976).

[33]The copper used in this experiment was from ASARCO.

[34]H. Alloul, Phys. Rev. Lett. 35, 460 (1975).

[35]K. G. Wilson, *Collective Properties of Physical Sytems*, *Nobel Symposium* 24 (Academic, New York, 1974); H. R. Krishna-Murthy, K. G. Wilson, and J. W. Wilkins, Phys. Rev. 35, 1101 (1975).